

Performance Enhancement of SnSe Thin Film Solar Cell Structure with ZnSe Buffer Layer Using SCAPS 1D

Md. Shakil Hussain ¹, Md. Rakibul Islam ²

¹ Department of Electrical and Electronic Engineering, Pundra University of Science & Technology, Bogura, Bangladesh

² Department of Electrical and Electronic Engineering, Pundra University of Science & Technology, Bogura, Bangladesh

Corresponding Author: Md. Shakil Hussain

Abstract: We simulated a device of solar cells that is based on Tin Selenide (SnSe) with configurations of standard planar (AZO/i-ZnO/CdS/SnSe/NiO) and (AZO/i-ZnO/ZnSe/SnSe/NiO) using the SCAPS-1D simulating software and compared several parameters of these solar cells. We used ZnSe instead of CdS to design the proposed cell, and it shows that the electrical properties of ultra-thin SnSe-based solar cells provide better characteristics along with the ZnSe buffer layer in comparison to the reported CdS buffer layer. The parameters of SnSe-based solar cells are investigated with the thickness of the absorber layer and buffer layer. The device used is CdSe, whose thickness is 1.2 μm , which has an optimum bandgap of 1.20 eV and a maximum efficiency of 22.69% with a VOC of 0.818 V, a short-circuit current density (JSC) of 33.65 mA cm^{-2} , and an FF of 82.41%. Finally, the proposed model achieved ZnSe-based solar cells with the highest PCE of 27.66%, a thickness of 0.06 μm , a VOC of 0.867 V, a JSC of 36.84 mA cm^{-2} , an FF of 86.4%.

Keywords: Window Layer, Buffer Layer, Window Layer-AZO, Buffer layer n- ZnSe tiling, Quantum Efficiency.

Date of Submission: 14-03-2024

Date of acceptance: 28-03-2024

I. INTRODUCTION

The modern world cannot be imagined for a second without electricity, which has now become the new parameter to determine the development status of a nation. We use a lot of electricity in almost all aspects of our daily lives. Electricity is used in household appliances, hospitals and medical care, transportation such as electric vehicles, driving heavy industrial machinery, all types of communication devices and the Internet, space equipment, entertainment, educational, and research purposes. In fact, electricity has now become an indicator of a country's development. Electricity is generated from both conventional and non-conventional energy sources (S.K. Deb, 1996). The present state of energy sources is shown in Figure 1.1.

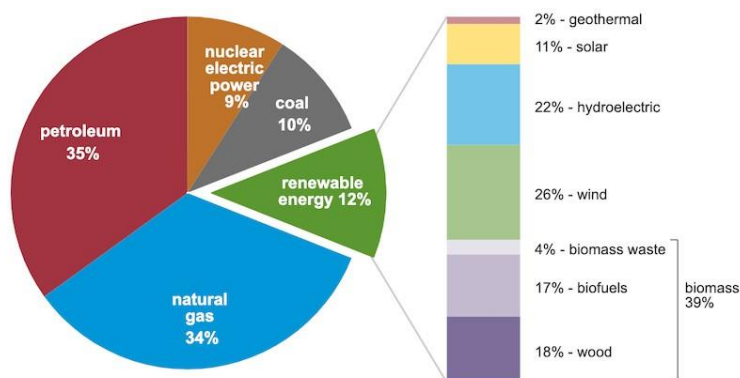


Figure 1.1: Present state of energy sources

Electricity is generated from these sources. The source wise generation scheme is shown in the below figure 1.2

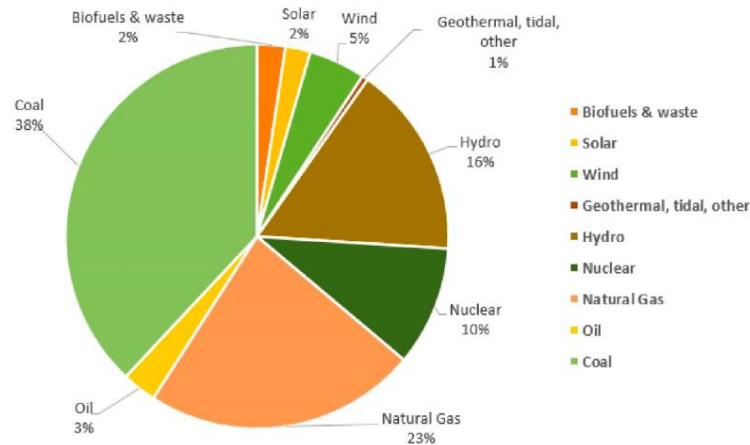


Figure 1.2: The source wise generation scheme

From the pie-chart it is seen that conventional sources dominate non-conventional to a great extent. But it is not all as some research shows that that non-conventional sources will lead in near future as conventional energy sources is highly discouraged due to their harmful effect to the environment. Country wise electricity demand is presented in the below figure 1.3.

II. SOLAR CELL PARAMETERS

The generation of electrical power from sunlight depends on different factors associated with a solar cell. These fabricated solar cells were characterized for parameters that can be extracted from I-V curves when the solar cell is subjected to illumination. The primary factors utilized to assess the efficiency of solar cells include:

- Open Circuit Voltage (V_{OC})
- Short Circuit Current (I_{SC})
- Short Circuit Current Density (J_{sc})
- Fill Factor (FF)
- Efficiency (η)
- Maximum Power Point (PM)
- Current at Maximum Power Point (I_M)
- The Voltage at Maximum Power Point (V_M)

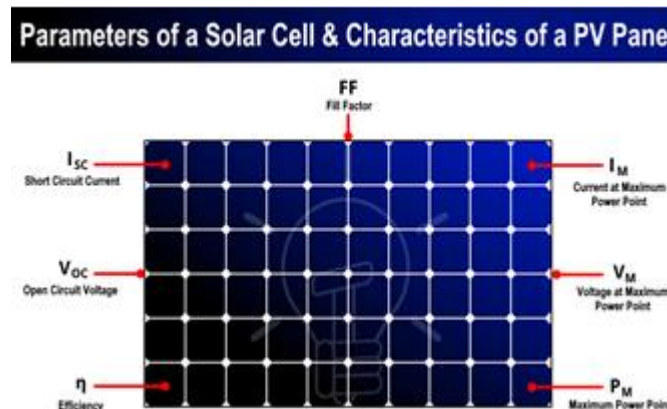


Figure 2.1: Parameters of solar cell.

2.1 Short Circuit Current (I_{SC})

Factors such as the area of the cell, solar radiation incident on the cell, cell technology, and other variables impact the short circuit value. At times, manufacturers might offer current density instead of the precise current value, denoted as "J," with the short circuit current density referred to as " J_{SC} ." Calculating the short circuit current density involves dividing the short circuit current by the solar cell's area, as shown below:

$$J_{sc} = I_{sc} / A$$

$$I_{sc} = I_{ph} - I_s e^{\frac{q(IR_s)}{AKT}} - 1$$

Where,

I_{sc} = Short circuit current,

I_{ph} = Photocurrent,

I_s = Diode reverse saturation current,

Q = Charge of an electron,

I = Cell current,

R_s = Series Resistance,

A = Ideality factor,

K = Boltzmann's constant,

T = Temperature in Kelvin

2.2 Open Circuit Voltage (V_{OC})

The open circuit voltage signifies the maximum voltage attainable by the cell under open-circuit conditions. V_{OC} 's magnitude is determined by both cell technology and the operating temperature of the cell. It is showed as the ratio of the maximum electrical power output to the radiation power input received by the cell, expressed as a percentage.

$$V_{oc} = \frac{nKT}{q} \ln \left(\frac{I_L}{I_o} + 1 \right)$$

Where,

V_{OC} = Open-circuit voltage,

I_o = Dark saturation current,

I_L = Light generated current,

n = identity factor,

T = temperature

III. MATERIALS USED FOR CONSTRUCTION OF SOLAR CELLS

Semiconductors play a crucial role in manufacturing solar cells, with silicon being the predominant material. Single-crystalline, multi-crystalline, and amorphous silicon are utilized in different configurations for construction.

Moreover, in the manufacturing of photovoltaic cells, polycrystalline thin films like copper indium di-selenide, cadmium telluride, and gallium arsenide are also employed.

➤ Silicon (Si):

Monocrystalline Silicon: Single crystal silicon wafers are used in monocrystalline solar cells, known for their high efficiency.

Polycrystalline Silicon: Multiple crystals make up polycrystalline silicon, and it is a cost-effective alternative to monocrystalline silicon (T. Saga et al., 2010).

➤ Thin-Film Technologies:

Amorphous Silicon (a-Si): Non-crystalline silicon used in thin-film solar cells for flexibility and ease of manufacturing (B. Xu et al., 2020).

Cadmium Telluride (CdTe): CdTe thin-film solar cells are known for their efficiency and cost-effectiveness (W.K. Metzger et al. 2019).

Copper Indium Gallium Selenide (CIGS): CIGS is another material used in thin-film solar cells, offering flexibility and good efficiency (J. Ramanujam et al., 2017; J. Ramanujam et al., 2020; A. Cho et al., 2021).

➤ Organic Photovoltaic Cells (OPV):

Organic Semiconductors: Carbon-based materials with conducting and semiconducting properties used in flexible and lightweight solar cells.

➤ Perovskite Solar Cells: Perovskite Materials: Hybrid organic-inorganic materials with a perovskite crystal structure have shown great promise in achieving high efficiency at a lower cost.

- **Dye-Sensitized Solar Cells (DSSC):**
Nanostructured Titanium Dioxide (TiO₂): Used as a semiconductor in DSSC, providing a large surface area for dye absorption (S.W. Lee et al., 2020).
Organic Dyes: Light-absorbing organic molecules that capture photons and generate an electric current.
- **Gallium Arsenide (GaAs):** Used in high-efficiency solar cells, especially in space applications due to its excellent performance under low-light conditions.
- **Copper-Indium-Gallium (CIG) Alloys:** Used in the development of high-efficiency thin-film solar cells.

3.1 Quantum Dots

Quantum dots, which are nanoparticles with a diameter of a few nanometers, are another type of developing material utilized in solar cells. Many typical elements used to make quantum dots, such as Cd and Pb, are poisonous, thus new compounds like copper indium selenide are being researched as alternatives (Z. Li et al., 2019).

3.2 Dye-Sensitized Materials

Another type of solar cell material is a small molecule dye, such as a ruthenium metalorganic dye, capable of absorbing a wide spectrum of visible light. The area for light absorption is increased by an inorganic mesoporous nanoparticle coating, commonly titanium dioxide (K.S. Gour et al., 2021).

3.3 Newer Materials

Current investigations have led to the emergence of several novel materials for solar cells. Nevertheless, a significant portion of these materials is still in the initial phases of exploration. Various compounds based on polymers and light-absorbing dyes, alongside inorganic elements, have been utilized in these advancements.

IV. WINDOW LAYER

The window layer within a solar cell is a thin material layer engineered to enable the passage of light while also establishing electrical contact with adjacent layers. Its main purpose is to mitigate the reflection of incoming light, which would otherwise diminish the solar cell's efficiency.

In addition, the window layer also serves as a protective layer, preventing contamination or damage to the underlying layers.

Various materials can serve as window layers in solar cells, selected based on the cell's specific needs. One prevalent choice is a thin film of amorphous silicon or microcrystalline silicon, commonly employed in thin-film solar cells. Alternatively, transparent conducting oxides (TCOs) like indium tin oxide (ITO) or fluorine-doped tin oxide (FTO) can also be utilized for this purpose (M. Hermle et al., 2020).

4.1 Transparent Conductive Oxide (TCO) layer

The Transparent Conductive Oxide (TCO) layer is an important component in the construction of a solar cell. It is typically made of a thin layer of a transparent conductive material such as indium tin oxide (ITO) or fluorine-doped tin oxide (FTO) that is deposited onto the surface of the solar cell.

The TCO layer serves two important functions in a solar cell. Firstly, it is responsible for transmitting the incident light to the active layer of the solar cell where the conversion of light into electrical energy takes place. Secondly, it acts as an electrical contact, allowing the flow of electrons out of the solar cell and into an external circuit.

4.2 Buffer Layer

In inexpensive thin-film solar cells, the buffer layer is positioned between the "window" and "absorber," constituting the pn junction of the solar cell. It facilitates the smooth transition between these layers. The buffer layer is employed to alleviate the conduction band offset, primarily reducing the electron flow from the absorber to the window and thereby minimizing efficiency losses. Additionally, it enhances the crystal quality of the solar cell and should possess the capability to accommodate higher doping densities. Functioning as an undoped region between the doped p-type and n-type layers of the solar cell, the buffer layer establishes a voltage difference between the two doped layers, enabling current flow from the p-type to the n-type and facilitating power generation.

4.3 Absorber Layer

The crucial element is the absorber layer, where both light absorption and carrier generation occur. The absorbing material's bandgap needs to be sufficiently small to capture a significant portion of the solar spectrum, yet large enough to minimize reverse saturation current density. Hence, direct bandgap semiconductors are the preferred choice. To ensure minimal loss during carrier transportation, it is essential for the minority carriers' diffusion length to be substantial. As a result, absorber layers predominantly consist of p-type semiconductors. In photovoltaic solar cells (PVSCs), the absorber layer functions as the perovskite layer, responsible for light absorption and the generation of free electrons and holes. The liberated charge carriers then undergo diffusion and drift, guided by an electric field (Y.H. Chang et al., 2021).

4.4 Back Contact

Back contact or rear contact of a solar cell eliminate shedding losses by putting both connections on the rear of the section. To establish a high-efficiency solar cell the back contact should have low resistance and low barrier. Various materials like Cu, Ni, Mo, Ag etc. are used as a back contact (C. Platzer-Björkman et al., 2017).

4.5 Glass Substrate

Glass substrate is mainly used to protect the solar photovoltaic cell against damaging external factors like water, vapor, and dirt. The current invention pertains to a glass substrate incorporated with a conductive film intended for use in solar cells. More precisely, it concerns a glass substrate featuring a conductive film that serves as an electrode substrate ideally suited for solar cell applications.

All Ibuprofen derivatives were effective in controlling the *Callosobruchus maculatus* pest, with mortality rates varying from 73% to 100%. It is possible to conclude that the derivatives produced have characteristics that are toxic to this species more pronounced than the drug that was the starting compound, ibuprofen, and therefore the study promotes results that may contribute to expand the stock of substances available for the control of pests, from the synthesis of the derivatives of ibuprofen. Important that studies that contribute to identify bioactive compounds produced from substances of permitted and consolidated use contribute to diversify the number of products used in pest control in order to obtain less toxic substances to man and environment and more selective in the specific combat of certain pests. As a result, the chemical synthesis reinforces its contribution to several sectors, including the pharmaceutical, agricultural and food industry, being decisive for the well-being of society and the environment.

V. METHODOLOGY

A. 5.1 Proposed Solar Cell Model

In our design, we have proposed a 5-layer solar cell comprising of AZO/i-ZnO/ZnSe/SnSe/NiO and to mention, we have taken Al (Aluminum) as the front contact and Glass/Mo (Molybdenum) as the back contact.

- Front Contact
- Window Layer (AZO)
- Transparent Conductive Oxide layer (i-ZnO)
- Buffer Layer (ZnSe)
- Absorber Layer (SnSe)
- Back Surface Field Layer (NiO)
- Back Contact

The structure of different layer is shown below to understand it easily:



Figure 5.1: Arrangement Of 5 Layer Thin film Solar Cell.

B. 5.2 The function of each layer

a) 5.2.1 Front contact-Al

Aluminum (Al) is a commonly used material for the front contact of solar cells, particularly in thin-film solar cells. The front contact in a solar cell is the layer that is in direct contact with sunlight and is responsible for absorbing the light and allowing it to be converted into electrical energy.

Aluminum is often preferred for the front contact in thin-film solar cells because it has a low resistivity and a high reflectivity, which means that it can efficiently collect and reflect light. Additionally, aluminum is relatively inexpensive and abundant, which makes it a cost-effective choice for large-scale solar cell production.

b) 5.2.2 Window Layer-AZO

The window layer in a solar cell is positioned between the front contact and the absorber layer, serving a vital function in the cell's operation. Its primary role is to permit sunlight to penetrate and reach the absorber layer, all the while offering a pathway with minimal resistance for the flow of electrical current. AZO (aluminum-doped zinc oxide) is a common material used for the window layer in solar cells. AZO is a transparent conductive oxide (TCO) material that is similar to the more well-known indium tin oxide (ITO), but it has several advantages over ITO. For example, AZO is less expensive and has better resistance to cracking and delamination than ITO.

In a solar cell, the AZO window layer is typically deposited onto a substrate using a technique such as sputtering or chemical vapor deposition. The thickness of the AZO layer can vary depending on the specific cell design and requirements, but it is usually in the range of a few hundred nanometers.

The AZO layer provides a number of important benefits to the solar cell, including:

- High transparency: AZO has a high optical transmittance, which means that it allows a large percentage of sunlight to pass through and reach the absorber layer.
- Low resistance: AZO has a low electrical resistance, which allows for efficient flow of electrical current through the cell.
- Good stability: AZO is chemically stable and does not degrade under the harsh conditions experienced in a solar cell.

Overall, the AZO window layer is an important component of many types of solar cells, and its properties play a key role in determining the efficiency and performance of the cell.

c) 5.2.3 Transparent Conductive Oxide Layer (i-ZnO)

The i-ZnO (intrinsic zinc oxide) layer is a type of layer used in this solar cells. It is positioned between the window layer and the absorber layer, and its main function is to act as a transparent conductive oxide (TCO) layer.

The i-ZnO layer is typically a thin layer of ZnO material that has been deposited onto a substrate using a technique such as sputtering or chemical vapor deposition. The layer is referred to as "intrinsic" because it is undoped, which means that it does not contain any impurities that would affect its electrical conductivity.

The i-ZnO layer has several important functions in a solar cell, including:

- High transparency: The i-ZnO layer is highly transparent to visible light, which means that it allows a large percentage of sunlight to pass through and reach the absorber layer.
- Low resistance: The i-ZnO layer has a low electrical resistance, which allows for efficient flow of electrical current through the cell.

- Good stability: The i-ZnO layer is chemically stable and does not degrade under the harsh conditions experienced in a solar cell.
- Energy band alignment: The i-ZnO layer helps to align the energy bands of the absorber layer and the window layer, which is important for efficient charge carrier generation and collection.

Overall, the i-ZnO layer is an important component of some types of solar cells, particularly those based on thin-film semiconductor materials. Its properties help to improve the efficiency and stability of the cell, and enable it to generate electrical energy from sunlight.

d) 5.2.4 Buffer layer n- ZnSe

The buffer layer within a solar cell is situated between the absorber layer and the window layer. Its main role is to serve as an intermediary between these two layers, facilitating a smooth transition between the distinct material properties utilized in the cell.

In certain solar cell configurations, particularly those utilizing thin-film semiconductor materials, the buffer layer consists of n-type ZnSe (zinc selenide) material. In such instances, the buffer layer is specifically termed as an n-ZnSe layer.

The n-ZnSe buffer layer has several important functions in a solar cell, including:

- Surface passivation: The n-ZnSe layer helps to passivate the surface of the absorber layer, which reduces the number of electronic defects and traps that can limit the performance of the cell.
- Energy band alignment: The n-ZnSe layer helps to align the energy bands of the absorber layer and the window layer, which is important for efficient charge carrier generation and collection.
- Electrical conductivity: The n-ZnSe layer is doped with impurities to make it electrically conductive, which allows for efficient flow of electrical current through the cell.

The thickness of the n-ZnSe buffer layer can vary depending on the specific design of the solar cell, but it is typically in the range of a few nanometers to a few hundred nanometers. The layer is typically deposited onto the absorber layer using a technique such as chemical vapor deposition or sputtering.

Overall, the n-ZnSe buffer layer plays a critical role in the performance of some types of solar cells, particularly those based on thin-film semiconductor materials. Its properties help to improve the efficiency and stability of the cell, and enable it to generate electrical energy from sunlight.

e) 5.2.5 Absorber Layer-SnSe

The absorber layer in a solar cell is the layer that is responsible for converting the energy of sunlight into electrical energy. In some types of solar cells, such as those based on thin-film semiconductor materials, the absorber layer is made of tin selenide (SnSe) material (S. Suresh et al., 2021).

SnSe is a semiconductor material that has several properties that make it well-suited for use as an absorber layer in solar cells. These properties include:

- High optical absorption: SnSe has a high absorption coefficient for sunlight in the visible and near-infrared parts of the spectrum, which means that it can efficiently convert sunlight into electrical energy.
- Good carrier mobility: SnSe has good electrical carrier mobility, which means that the charge carriers generated by the absorption of sunlight can move easily through the material.
- Earth-abundant and non-toxic: SnSe is made of abundant and non-toxic elements, which makes it an attractive alternative to other absorber materials that contain rare or toxic elements.

The SnSe absorber layer is typically deposited onto the buffer layer using a technique such as sputtering or thermal evaporation. The thickness of the layer can vary depending on the specific design of the solar cell, but it is typically in the range of a few hundred nanometers to a few micrometers.

Overall, the SnSe absorber layer is an important component of some types of solar cells, particularly those based on thin-film semiconductor materials. Its properties help to improve the efficiency and stability of the cell, and enable it to generate electrical energy from sunlight.

f) 5.2.6 Back contact- Glass/Mo

The back contact of a solar cell is tasked with collecting the electrical current produced by the absorber layer and conveying it out of the cell. In certain solar cell configurations, particularly those employing thin-film technology, the back contact consists of a glass layer coated with a layer of molybdenum (Mo) (V. Karade et al., 2019).

The glass/Mo back contact offers several key properties that render it highly suitable for solar cell applications, including:

- High electrical conductivity: The molybdenum layer is highly conductive to electricity, which allows for efficient collection and transport of the electrical current generated by the cell.
- Chemical stability: Both glass and molybdenum are chemically stable materials that do not degrade over time, which ensures the long-term stability and durability of the solar cell.
- Good adhesion: The molybdenum layer adheres well to the glass substrate, which helps to prevent delamination or other types of mechanical failure in the cell.

- **Low reflectivity:** The glass substrate has low reflectivity, which allows for more sunlight to be absorbed by the absorber layer and converted into electrical energy.

The glass/Mo back contact is typically deposited onto the absorber layer using a technique such as sputtering or chemical vapor deposition. The thickness of the molybdenum layer can vary depending on the specific design of the solar cell, but it is typically in the range of a few hundred nanometers to a few micrometers.

In summary, the glass/Mo back contact plays a pivotal role in specific types of solar cells, especially those utilizing thin-film technology. Its unique properties contribute to enhancing the efficiency and stability of the cell, facilitating the conversion of sunlight into electrical energy.

C. 5.3 Work Flow Analysis

In this thesis we have performed all analysis through scaps-1d software. Whole working is shown in the work flow diagram bellow.

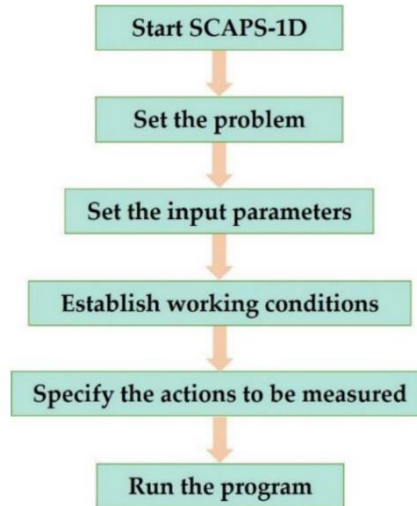


Figure 5.2: Work flow diagram

Initially, we initiated the use of the scaps-1d software. Here, the Standard Test Conditions (STC) for photovoltaic (PV) systems are employed as a standardized benchmark, allowing for comparison across various devices, including those developed in research and commercial PV panels as depicted in Figure 5.1. These conditions entail measurements taken at a temperature (T) of 300 K, atmospheric pressure of 1 atm., and exposure to an AM.1.5G irradiance spectrum, which corresponds to a power density of 1 kW m^{-2} . Then we clicked in the Set Problem button to add all the parameters used in this thesis paper.

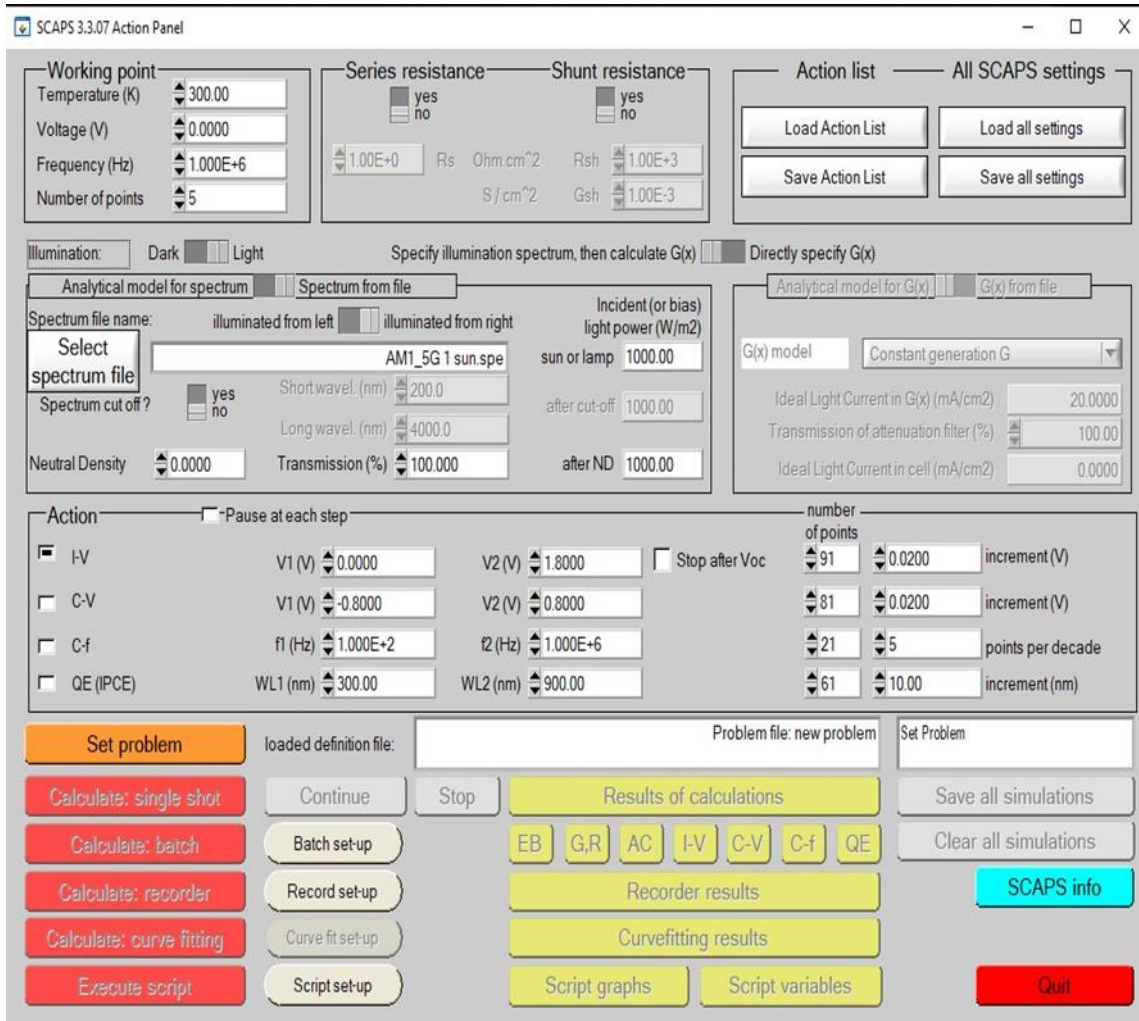


Figure 5.3: Set work condition, illumination condition and set problem

From action panel we have selected i-v to see i-v characteristics, open circuit voltage (V_{oc}), short circuit current (J_{sc}), Fill factor (FF) and power conversion efficiency (PCE) of simulated solar cell. We have set the illumination condition as light shown in the figure 5.2.

We have set the problem by selecting on set problem on which we set up solar cell structure shown in the figure 5.3.

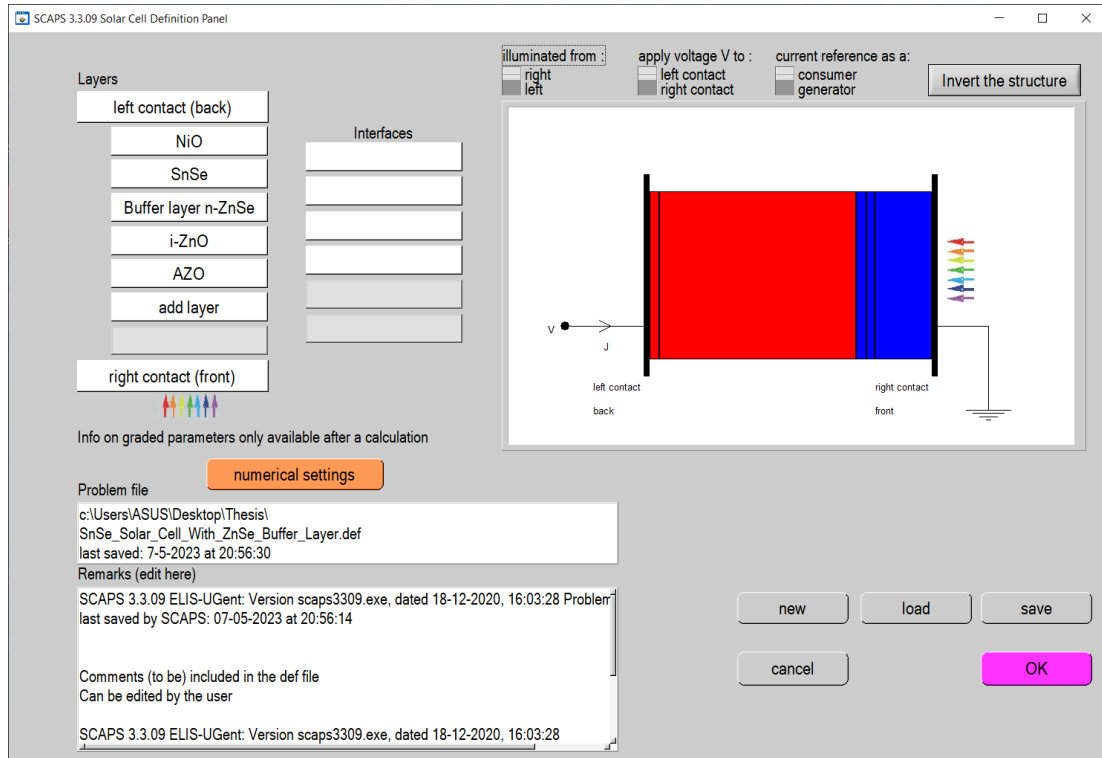


Figure 5.4: Set solar cell structure then we have set each layer parameter.

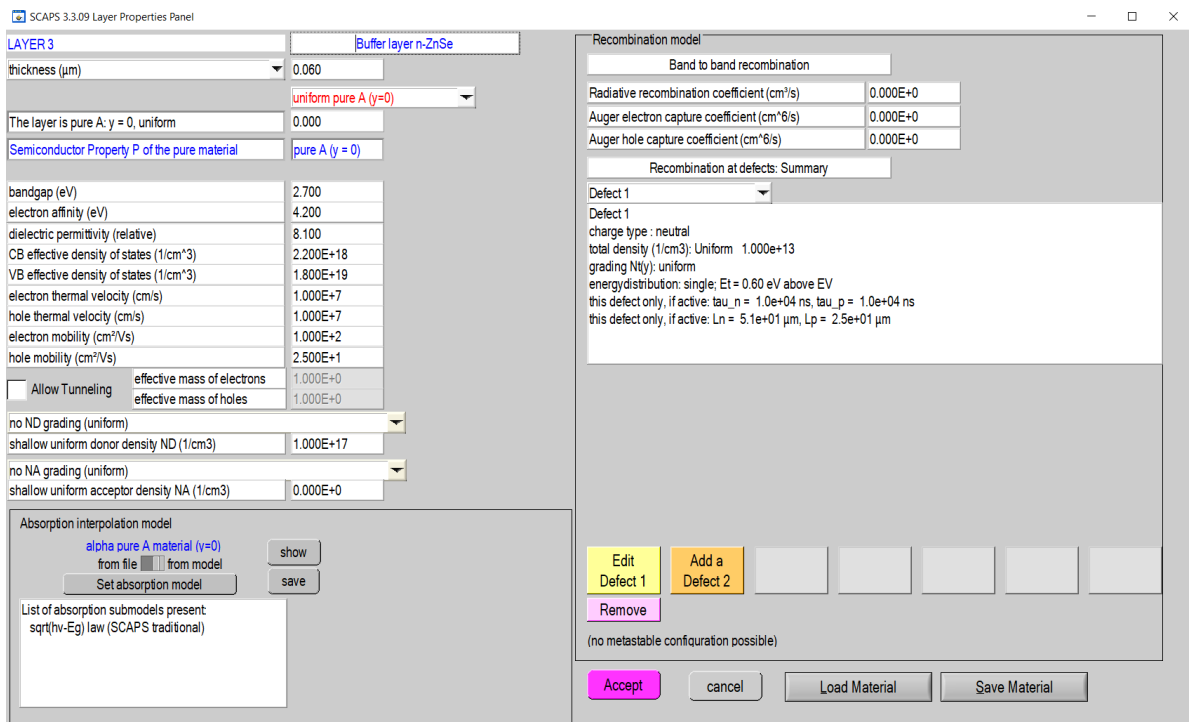


Figure 5.5: Set material specification

Table 5.1 Here are the physical parameters of the materials NiO, SnSe, ZnSe, i-ZnO, and AZO typically used for simulating the Mo/NiO/SnSe/ZnSe/i-ZnO/AZO/Al heterojunction solar cell:

Table 5.1 Physical parameters of used material

Parameters	NiO	SnSe	ZnSe	i-ZnO	AZO
Thickness (nm)	Variable	1200	60	50	350
Bandgap	3.8	1.2	2.7	3.4	3.6
Electron affinity (eV)	1.46	4.20	4.20	4.55	4.50
Dielectric permittivity (relative)	10.07	12.50	8.10	09.00	09.00
CB effective density of state (cm ⁻³)	2.8×10^{19}	1.75×10^{18}	2.2×10^{18}	2.2×10^{18}	2.2×10^{18}
VB effective density of state (cm ⁻³)	1×10^{19}	4.57×10^{18}	1.8×10^{19}	1.8×10^{19}	1.0×10^{19}
Mobility of electron (cm ² V ⁻¹ s ⁻¹)	130	130	100	100	100
Mobility of hole (cm ² V ⁻¹ s ⁻¹)	56.7	56.7	25.0	25.0	25.0
Shallow donor density ND (cm ⁻³)	107	0	1.0×10^{17}	1.0×10^{18}	1.0×10^{20}
Shallow acceptor density NA (cm ⁻³)	2.80×10^{19}	1.75×10^{16}	0	0	0
Thermal velocity of electron (cm s ⁻¹)	107	107	107	107	107
Thermal velocity of hole (cm s ⁻¹)	107	107	107	107	107
Nt (cm ⁻³)	1.0×10^{14}	1.0×10^{16}	8.8×10^{16}	1.0×10^{14}	3.0×10^{16}
Coefficient of radiative recombination (cm ³ s ⁻¹)	2.3×10^{-9}	2.3×10^{-9}	2.3×10^{-9}	2.3×10^{-9}	2.3×10^{-9}
Absorption coefficient	Data file	default	default	default	default

Table 5.2 Physical properties utilized in simulating the top and bottom contacts.

Contact	Back (Mo)	Front (Al)
Thickness	1000 nm	1000 nm
Alignment/work function	4.9 eV	4.2 eV
S_e	105 cm s ⁻¹	105 cm s ⁻¹
S_h	107 cm s ⁻¹	107 cm s ⁻¹
Tunneling	No	No
Reflection	No	Yes

VI. RESULT AND DISCUSSION

A. 6.1 I-V Characteristics Curve of Our Proposed Solar Panel

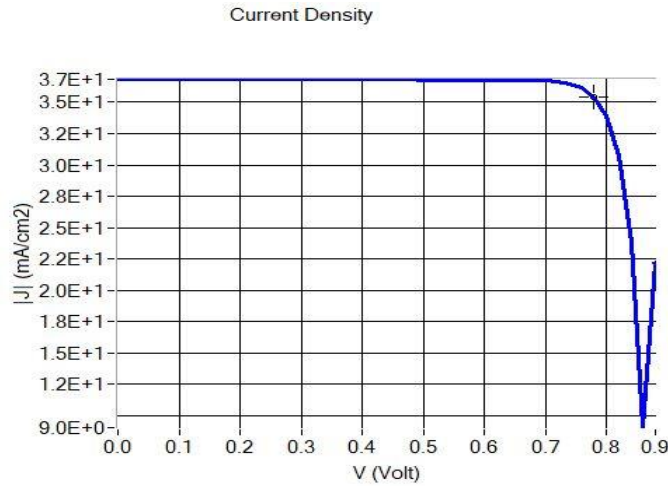


Figure 6.1: I-V Characteristics Curve of Our Proposed Solar Panel

The characteristics curve is significant to understand the performance of a solar panel. It reveals so many details about the solar cell. It displays graphs of output voltage versus current on various levels. We can calculate the power rating of a solar cell by taking a look at this curve. It plays a crucial role in determining the output performance of the device and the efficiency of solar energy conversion. It serves as a visual depiction of the operation of solar panels in the industry. Based on the IV characteristic curve of the proposed solar cell, we have achieved an open circuit voltage exceeding 0.8 V and a current density of approximately 36 mA/cm².

B. 6.2. Quantum Efficiency (QE)

The Quantum efficiency of a solar cell is the ratio of collected carriers to the incident photons at the cell's specific energy. The external quantum efficiency plot, depicted in the figure, takes into account optical losses like reflection and transmission. However, the internal quantum efficiency does not consider these losses. Analyzing both plots at different depths into the wafer provides insights into cell performance. A diminished response in the red wavelength region suggests carrier loss in the bulk or due to inadequate backside contact. When all photons of a particular wavelength are absorbed, and the resulting minority carriers are successfully collected, the Quantum Efficiency for that specific wavelength is unity.

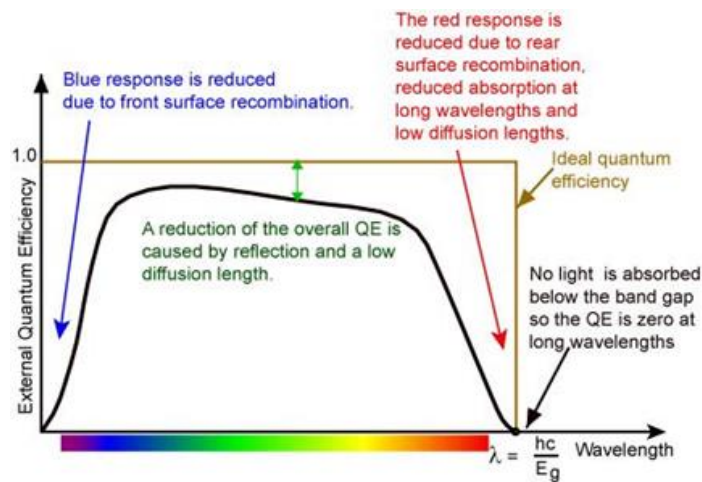


Figure 6.2: Quantum Efficiency at Various Wavelength

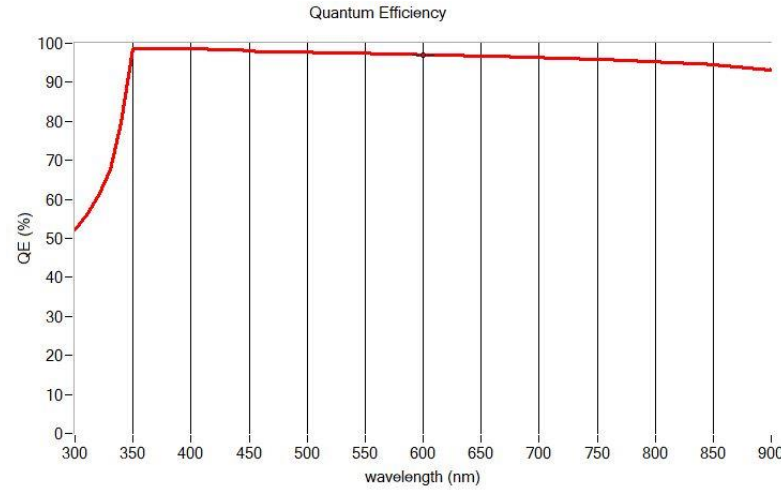


Figure 6.3: Quantum Efficiency of ZnSe Based Solar Cell.

By assessing the curves in Figure 6.3, we can see that the Quantum Efficiency of ZnSe is much more stable, which has a direct positive impact on the performance of our proposed solar panel.

C. 6.3 Thickness Variation of NiO Layer on Various Parameters

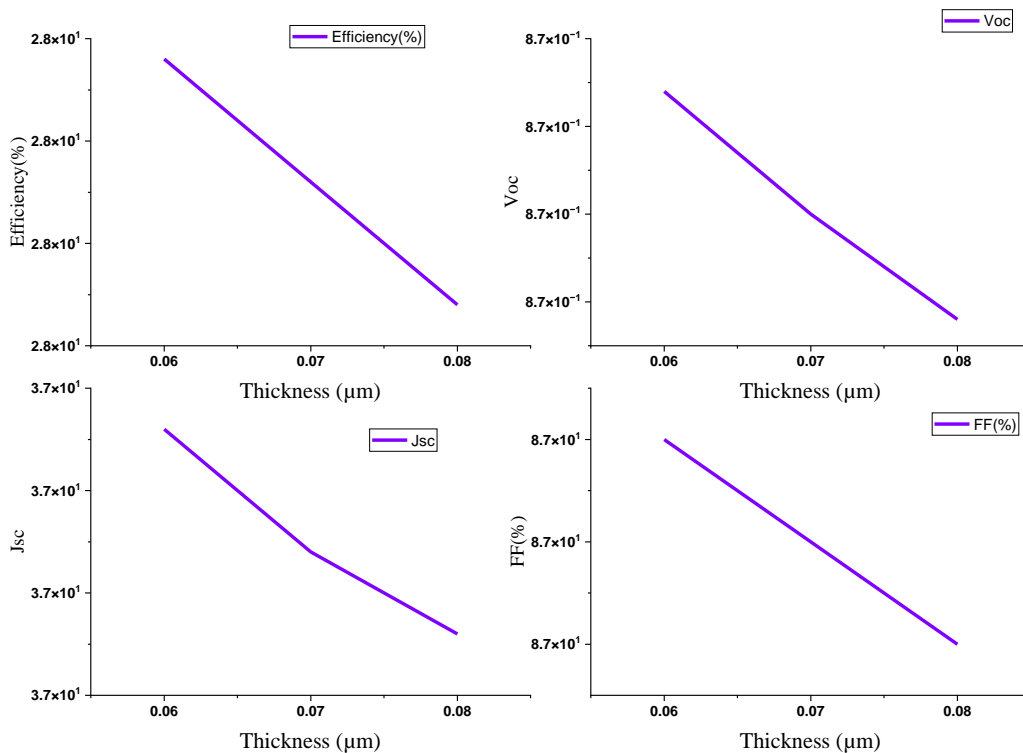


Figure 6.4: Thickness of NiO vs Other Parameters

In the figure 6.4, we can see for the first quadrant (a) that when we increased the thickness of the NiO layer, the efficiency decreases gradually, the 2nd quadrant, we have observed that Voc decrease for 0.06 μm to 0.08 μm . At the 3rd quadrant, we have got the same value of current density from the thickness 0.06 μm 0.08 μm , then it decreases gradually. At the 4th quadrant, we notice that fill factor decreases until 0.06 μm and remain the same until 0.08 μm . We can say from above discussion the thickness 0.06 μm is suitable to get out desired parameters value [Voc, Jsc, FF(%), Eff(%)].

D. 6.4 Thickness Variation of SnSe Layer on Various Parameters

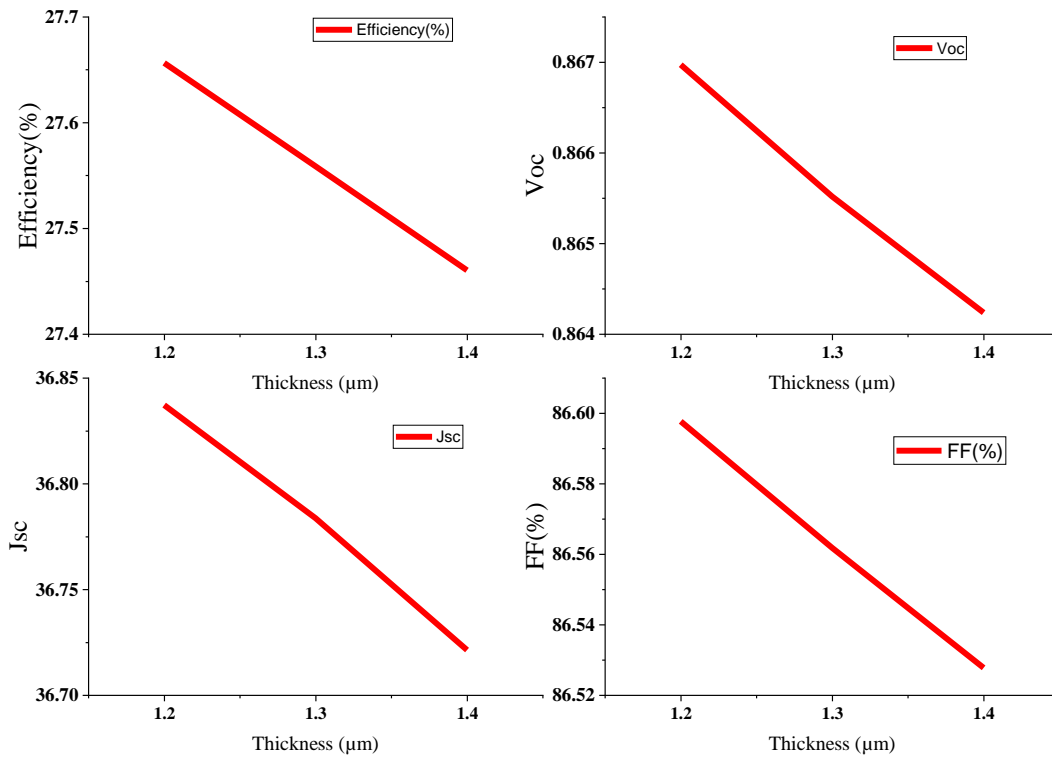


Figure 6.5: Thickness of SnSe vs Other Parameters

In Figure 6.5, we have tried to show the differences that occurred when the thickness of the absorber layer (SnSe) was changed. We see for thicknesses 1.2 μm give best efficiency. In the second quadrant, the open-circuit voltage continuously down as the thickness of the absorber layer raised, and we hit our maximum Voc at 1.2 μm thickness. In the third quadrant, we have seen that the short circuit current decreases gradually and we have obtained the maximum value of 36.42 mA/cm² for the thickness of 1.2 μm of SnSe. At the 4th quadrant, we notice that the Fill factor (%) increases as the thickness increases and we have got the same value for 1.2 μm and 1.4 μm and a maximum value for 1.2 μm , which is 86.60. We have obtained the maximum efficiency of 27.66 for the thickness of 1.2 μm . So, after the observation, we have taken the thickness of SnSe is 1.2 μm .

E. 6.5 Thickness Variation of ZnSe Layer on Various Parameters

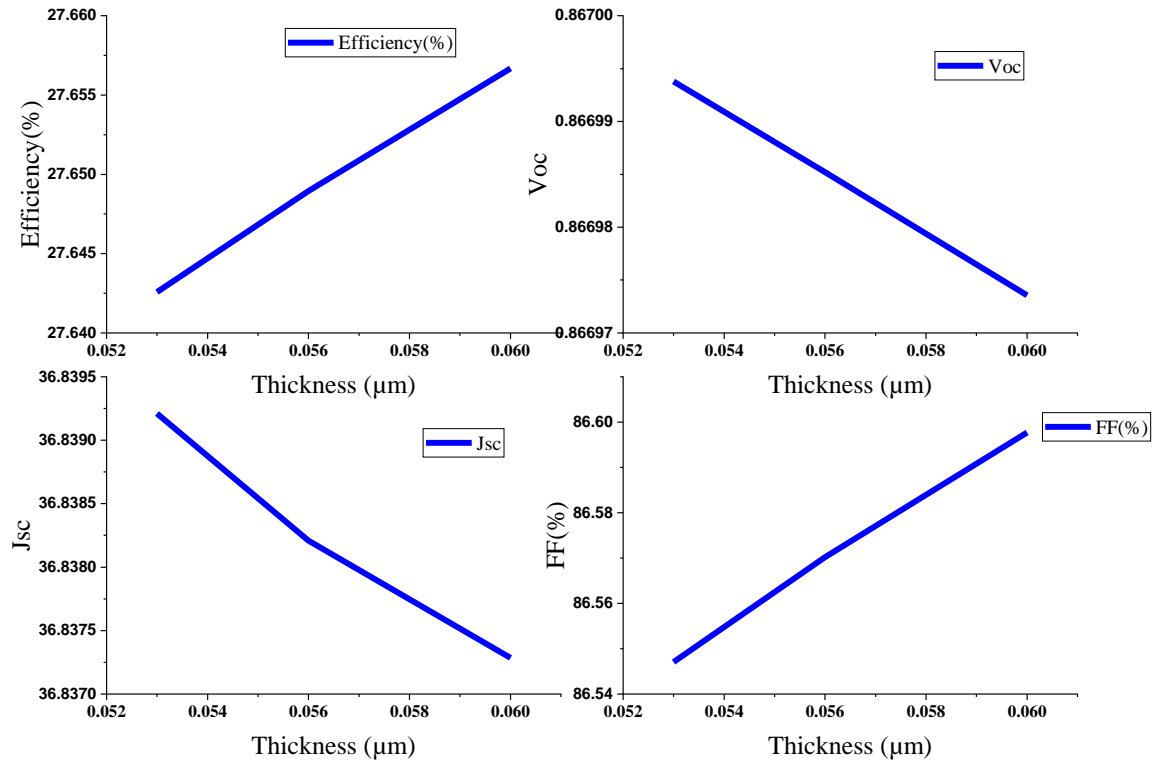


Figure 6.6: Thickness of ZnSe vs Other Parameters

In the figure 6.6, we have observed that Voc value decrease for 0.052 μm to 0.06 μm. At the 3rd quadrant, we have observed that decreases value of current density from the thickness 0.052 μm 0.06 μm, gradually. At the 4th quadrant, we notice that fill factor increases until 0.052 μm and remain the same until 0.06 μm. We can say from above discussion the thickness 0.06 μm is suitable to get out desired parameters value [Voc, Jsc, FF (%), Eff (%)].

F. 6.6 Discussion

From above analysis, we have chosen some relevant values, and here we are going to explore the result and make a decision. So, the solar panel offers better output. The taken values are shown below:

Table 6.1: Outcome

Open circuit Voltage (V)	Short Circuit Current density (ma/cm ²)	Fill Factor (%)	Efficiency (%)	Nº of layer used
0.8670	36.837286	86.60	27.66	5

G. 6.7 Comparison between Proposed Solar Panel & Reported Solar Panel

Table 6.2: Comparison between CdS and ZnSe based solar cell

Parameters	Reported solar cell (AZO/i-ZnO/CdS/SnSe/NiO)	Proposed Solar cell (AZO/i-ZnO/ZnSe/SnSe/NiO)
Voc (V)	0.818	0.8670
Jsc (mA/cm ²)	33.65	36.84
FF (%)	82.41	86.60
Eff (%)	22.69	27.66

Table 6.2 shows the comparison of results with the reported and proposed structure. Our proposed structure successfully achieved a higher value in all parameters, a good sign of being an excellent solar panel. While the reported solar panel is finding it tough to sustain, our proposal can address those without difficulty. Here in all the segments our proposed solar cell managed to outpace the trending SnSe/CdS based solar cell and stay triumphed. Using ZnSe in place of CdS has brought to us much improvements, stability and environment friendly solar cell. So hopefully the results do justice to our proposed solar cell.

VII. CONCLUSION

We attempted to demonstrate the solar energy process, the function of the solar cell, the effectiveness of our proposed solar cell, how efficiency can be improved, methods for building a better, globally oriented solar cell, the designing process, and why solar cells will lead in the future in this paper. Our suggestion will surely have a substantial impact both now and in the future.

The electrical attributes of ultra-thin solar cells based on SnSe exhibit improved characteristics, especially when coupled with a ZnSe buffer layer, surpassing those reported for CdS buffer layers. The parameters of SnSe-based solar cells have been systematically studied in relation to both the absorber layer and the buffer layer thickness. The optimal thickness chosen for the SnSe absorber layer is 1.2 μm , offering an ideal bandgap of 1.20 eV. Through this configuration, a ZnSe-based solar cell has been successfully developed, achieving a peak efficiency of approximately 27.66% with a buffer layer thickness of 0.06 μm .

REFERENCES

- [1]. S.K. Deb, Thin-film solar cells: An overview, *Renewable Energy*, 8 (1996) 375- 379,[https://doi.org/10.1016/0960-1481\(96\)88881-1](https://doi.org/10.1016/0960-1481(96)88881-1).
- [2]. V. Karade, A. Lokhande, P. Babar, M.G. Gang, M. Suryawanshi, P. Patil, J.H. Kim, Insights into kesterite's back contact interface: A status review, *Sol. Energy Mater. Sol. Cells*, 200 (2019) 109911,<https://doi.org/10.1016/j.solmat.2019.04.033>.
- [3]. M. Hermle, F. Feldmann, M. Bivour, J.C. Goldschmidt, S.W. Glunz, Passivating contacts and tandem concepts: Approaches for the highest silicon-based solar cell efficiencies, *Appl. Phys. Rev.*, 7 (2020) 021305,<https://doi.org/10.1063/1.5139202>.
- [4]. T. Saga, *Advances in Crystalline Silicon Solar Cell Technology for Industrial Mass Production* NPG Asia Materials 2, 96-102 (2010), in, 2010,<http://dx.doi.org/10.1038/asiamat.2010.82>.
- [5]. J. Ramanujam, U.P. Singh, Copper indium gallium selenide based solar cells—a review, *Energy Environ. Sci.*, 10 (2017) 1306-1319,<https://doi.org/10.1039/C7EE00826K>.
- [6]. W.K. Metzger, S. Grover, D. Lu, E. Colegrove, J. Moseley, C. Perkins, X. Li, R. Mallick, W. Zhang, R. Malik, Exceeding 20% efficiency with in situ group V doping in polycrystalline CdTe solar cells, *Nat. Energy*, 4 (2019) 837-845,<https://doi.org/10.1038/s41560-019-0446-7>.
- [7]. S.W. Lee, S. Bae, D. Kim, H.S. Lee, Historical Analysis of High- Efficiency, Large- Area Solar Cells: Toward Upscaling of Perovskite Solar Cells, *Adv. Mater.*, 32 (2020) 2002202,<https://doi.org/10.1002/adma.202002202>.
- [8]. J. Ramanujam, D.M. Bishop, T.K. Todorov, O. Gunawan, J. Rath, R. Nekovei, E. Artegiani, A. Romeo, Flexible CIGS, CdTe and a-Si: H based thin film solar cells: A review, *Prog. Mater. Sci.*, 110 (2020) 100619,<https://doi.org/10.1016/j.pmatsci.2019.100619>.
- [9]. A. Cho, I. Jeong, S. Song, D. Shin, S. Lee, K. Kim, J.H. Yun, J.S. Cho, J.H. Park, Mechanism- Based Approach of CdS/Cu (In, Ga) Se₂ (CIGS) Interfaces for CIGS Solar Cells through Deposition in Different Stages of Continuous Chemical Bath Deposition Reaction: Key to Achieving High Photovoltaic Performance, *Sol. RRL*, 5 (2021) 2100485,<https://doi.org/10.1002/solr.202100485>.
- [10]. S. Suresh, A.R. Uhl, Present Status of Solution- Processing Routes for Cu (In, Ga)(S, Se)₂ Solar Cell Absorbers, *Adv. Energy Mater.*, 11 (2021) 2003743, <https://doi.org/10.1002/aenm.202003743>.
- [11]. Y.H. Chang, R. Carron, M. Ochoa, C. Bozal- Ginesta, A.N. Tiwari, J.R. Durrant, L. Steier, Insights from Transient Absorption Spectroscopy into Electron Dynamics Along the Ga- Gradient in Cu (In, Ga) Se₂ Solar Cells, *Adv. Energy Mater.*, 11 (2021) 2003446,<https://doi.org/10.1002/aenm.202003446>.
- [12]. C. Platzer-Björkman, Kesterite compound semiconductors for thin film solar cells, *Curr. Opin. Green Sustain. Chem.*, 4 (2017) 84-90,<https://doi.org/10.1016/j.cogsc.2017.02.010>.
- [13]. K.S. Gour, V. Karade, P. Babar, J. Park, D.M. Lee, V.N. Singh, J.H. Kim, Potential Role of Kesterites in Development of Earth- Abundant Elements- Based Next Generation Technology, *Sol. RRL*, 5 (2021) 2000815,<https://doi.org/10.1002/solr.202000815>.
- [14]. B. Xu, C. Ma, X. Lu, Y. Liu, Q. Zhang, Y. Chen, P. Yang, J. Chu, L. Sun, Beyond 10% efficient Cu₂ZnSn (S, Se) 4 solar cells: Effects of the introduction of SnS powder during selenization process, *Sol. Energy Mater. Sol. Cells*, 210 (2020) 110522,<https://doi.org/10.1016/j.solmat.2020.110522>.
- [15]. Z. Li, X. Liang, G. Li, H. Liu, H. Zhang, J. Guo, J. Chen, K. Shen, X. San, W. Yu, 9.2% - efficient core-shell structured antimony selenide nanorod array solar cells, *Nat. Commun.*, 10 (2019) 1-9,<https://doi.org/10.1038/s41467-018-07903-6>.